Chemosphere 170 (2017) 17–24

Contents lists available at ScienceDirect

Chemosphere

journal homepage: www.elsevier.com/locate/chemosphere

Spatial distribution and transport characteristics of heavy metals around an antimony mine area in central China

Xin Li [a, b, *], Hong Yang [a, b], Chang Zhang [a, b], Guangming Zeng [a, b], Yunguo Liu [a, b], Weihua Xu [a, b], Youe Wu [a, b], Shiming Lan [a, b]

[a] College of Environmental Science and Engineering, Hunan University, Changsha 410082, PR China
[b] Key Laboratory of Environmental Biology and Pollution Control (Hunan University), Ministry of Education, Changsha 410082, PR China

HIGHLIGHTS

- As and Sb showed similar geochemical behavior on transport and deposition.
- Lower concentrations for Cr, Mn and Ni may be controlled by natural factors.
- Cu, Zn, Cd and Pb may be released from sulfide minerals.
- Heavy metal distribution trends were associated with local wind direction.
- The environment quality was obviously threatened by accumulation of Sb and Cd.

GRAPHICAL ABSTRACT

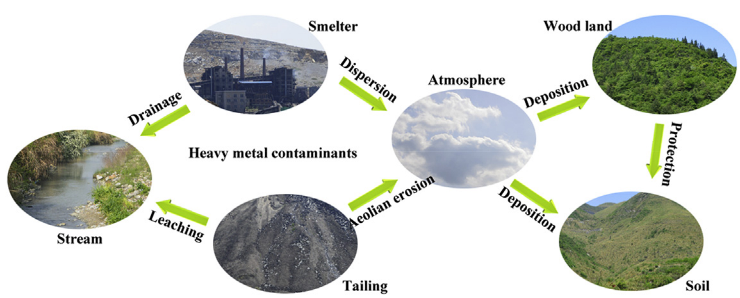

ARTICLE INFO

Article history:
Received 15 July 2016
Received in revised form
2 December 2016
Accepted 4 December 2016
Available online 7 December 2016

Handling editor: Martine Leermakers

Keywords:
Heavy metals
Sources
Aeolian erosion
Spatial distribution
Pollution degree

ABSTRACT

The spatial distribution and transport characteristics of heavy metals in an antimony mine area (Xikuangshan, China) were systematically studied using a field survey and geostatistical analytical methods. In the study area, 52 soil and sediment samples were collected from bare land, grassland, woodland and river sediments covering a surface area of 20 km^2. The soil properties and heavy metal concentrations were measured by wavelength dispersive X-ray fluorescence spectrometry and inductively coupled plasma-mass spectrometry, respectively. Correlation analysis and principal component analysis suggest that Cu, Zn, Cd, As, Pb and Sb can be attributed to anthropogenic inputs, whereas Cr, Mn and Ni are of natural origin. Distribution maps of heavy metals were generated using the Kriging interpolation method to identify their distribution trends. The results show the influence of wind, river, distance and vegetation on the spatial distribution. The results also revealed that windborne transport may play a significant role in the spreading of contaminants. In addition, the environmental risk of heavy metal pollution was evaluated using their geoaccumulation indexes in the whole region. All of the results indicate that the heavy metal distributions in the soils were consistent with the local prevailing wind direction. In addition, the environmental quality could be seriously threatened by heavy metal contaminants from the smelter and tailings.

1. Introduction

For historical and current nonferrous metal mining and smelting

* Corresponding author. College of Environmental Science and Engineering, Hunan University, Changsha 410082, PR China.
E-mail address: hgxlixin@hnu.edu.cn (X. Li).

http://dx.doi.org/10.1016/j.chemosphere.2016.12.011
0045-6535/© 2016 Published by Elsevier Ltd.

districts, heavy metal pollution should be the top environmental issue. Anthropogenic activities such as the extraction, beneficiation processes and smelting of metal ores have produced large quantities of mine wastes that contain a number of heavy metals. These mine wastes may disperse more easily and rapidly into the environment than coarser ores (Csavina et al., 2011). In many regions, they have been transported by weathering and erosion, resulting in the spatial distribution of heavy metals (Kim et al., 2014). Heavy metals are released into the proximal atmosphere, fluvial and soil systems, causing adverse impacts on ecosystems (Fu et al., 2016).

The mobilization of metal-bearing mine wastes can be expected to elevate metal concentrations in soils as a result of the aeolian erosion of mine tailings. In addition, the weathering of parent rocks is also a major source of heavy metals in soils (de Souza et al., 2015). The contributions of heavy metals in soils should be identified to control their mobilization. Considering the complex sources of heavy metals, principal component analyses are usually applied to distinguish their natural sources and anthropogenic inputs in soil pollution surveys (Szolnoki et al., 2013). Furthermore, some studies have found that multivariate statistics analyses are an effective method for considering the relationship among variables (Dragović et al., 2008).

Elevated concentrations of heavy metals in soils, water, plants and food chains can result in severe environmental issues (Calace et al., 2005). Environmental pollution risks can usually be estimated using the spatial interpolation method (Sun et al., 2013). Consequently, the method of spatial interpolation has been applied in studies of heavy metals transport tendencies and potential risk area assessments (Li et al., 2013). However, a variety of factors such as distance and vegetation significantly influence the mobility and deposition of fine particulates (Chopin and Alloway, 2007; Křibek et al., 2014). More attention should therefore be paid to investigate factors that could control fine particulate transport and distribution in study areas.

Xikuangshan is known worldwide for its antimony minerals and tremendous production. Since the 1890s, larger amounts of antimony ores have been exploited (Liu et al., 2010). Long-term antimony mining and smelting have led to very serious heavy metal pollution. Earlier researchers have undertaken a large amount of work on the distribution and sources of heavy metals in this area (Okkenhaug et al., 2011; Wang et al., 2011). However, few studies have been conducted on the windborne transport of heavy metal contaminants. The objective of this investigation was to discuss the distribution and transport characteristics of heavy metals using a soil and sediment survey of the study area. The main aims of this study were (1) to reveal the influences of wind, distance, river and vegetation on the transport and distribution of heavy metals, (2) highlight the relationship between heavy metal transport tendencies and prevailing wind directions and (3) evaluate the potential risks of heavy metal pollution in the area. The results of this research will provide a basis for monitoring the tracks of heavy metal migration in the mining area and can also be used to protect soils from the long-term accumulation of heavy metals.

2. Materials and methods

2.1. Study area

Xikuangshan is located in the vicinity of Lengshuijiang city, Hunan Province, central China (Fig. 1). The locality is a suburb in mountain areas and is distributed over an area of 20 km^2. The area is one of the oldest and best-known mining districts worldwide due to its incomparably rich deposits of antimony minerals. As much as approximately 40 million tons of antimony reserves remain after hundreds of years of exploration (Qi et al., 2011). In most of the antimony-rich deposits, stibnite (Sb_2S_3) is the primary ore mineral. The stibnite is accompanied by pyrite (FeS_2), arsenopyrite (FeAsS), sphalerite (ZnS), and galena (PbS) (Yang et al., 2006). There are many smelters adjacent to the mining area, including antimony, lead and zinc smelters. Mining related activities have generated large amounts of tailings and smelting waste. These industrial wastes occur over an extensive area and have been subjected to water runoff and aeolian erosion for many years, and as a consequence they pose large threats to the entire region (Yang et al., 2015).

The area's climate is typically subtropical monsoon. The average annual temperature, wind speed and precipitation are 16.8 °C, 1.6 m/s and 1354 mm, respectively. The rainy season primarily occurs during March to August. The prevailing wind direction is primarily NW, with increased NNE and WWN components in the study area (Fig. S1, Electronic Supplementary Material).

2.2. Sample collection and treatment

A total of 52 sampling sites were distributed over the study area, primarily according to the grid distribution point method, with 13 sites in woodlands, 22 sites in grassland, 12 sites in bare land and 5 sites in river sediments, respectively (Fig. 1). To obtain highly detailed information, the sampling density was increased in areas under the prevailing wind direction and close to piles of mine tailings. However, the sampling sites were placed far from interference areas such as roads, residential districts and cultivated land. Five stream sediment samples were collected along the stream flow direction. After removing the organic horizons, four subsamples (5–15 cm depth) were collected and mixed from four points within 5 m radii of the sampling sites (Sajn, 2006). Eventually, the location of one collected sample site was recorded using the Global Position System (GPS), with 10 m precision. Approximately 1.0 kg of each sample were stored in polyethylene bags using stainless spatula and transported to the laboratory.

The collected samples were air-dried indoors, disaggregated and homogenized with a porcelain and pestle, and sifted through a 2 mm nylon sieve to remove extraneous material. For the chemical analyses, a portion of the sieved soil was milled in an agate mill. It was then pulverized to an adequate size (<0.15 mm) for digestion and to measure the heavy metal concentrations. The <2 mm sediment fraction was sieved to less than 0.125 mm for instrumental analysis. Soil and sediment samples (<2 mm) were used for the pH measurements. To obtain subsamples, all the samples were placed in an oven at 105 °C for 1 h and then 60 °C to a constant weight.

2.3. Sample analysis

The soil and sediment sample parameters were analyzed for pH, sulfide and heavy metals (Cr, Mn, Ni, Cu, Zn, As, Cd, Pb and Sb). The pH values were measured using a pH meter equipped with 1:2.5 (V/V) sample suspension in deionized water using a glass electrode. The amounts of total S (%) were directly determined by wavelength dispersive X-ray fluorescence spectrometry analysis (XRF, PANalytical Axios^{mAX} apparatus).

The metal concentrations were determined following standard procedures (ISO11047, 1998). Briefly, 0.25 g of dry sample was accurately weighed in a Teflon digestion vessel with 12 mL aqua regia (a mixture of 69% HNO_3 and 37% HCl at 1:3 v/v). Subsequently, the samples were digested on a graphitic panel heater for 2 h. Once the digestion was completed, the extracts were cooled, filtered and diluted to 50 mL to separate some insoluble silicate particles. The total metal concentrations in the extracts were determined using an inductively coupled plasma mass spectrometer (ICP-MS, Agilent 7700 series). For analyzing the heavy metal concentrations in the

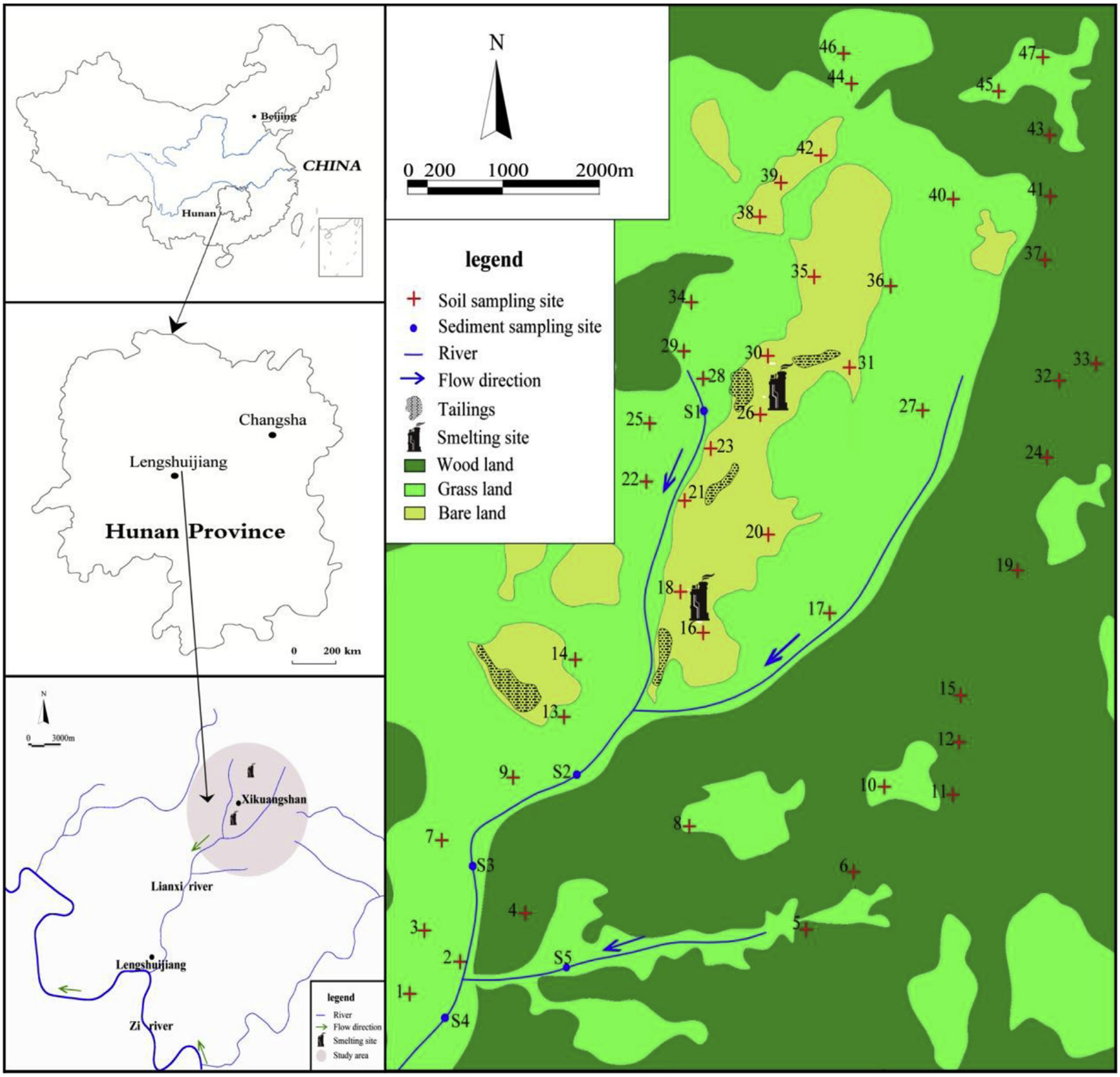

Fig. 1. Simplified map of the study area and sampling location of soil and river sediment.

soil and sediment samples, the accuracy of the analytical procedures was checked using duplicates, blanks and standard reference materials (GBW07305, GBW07405, Shenzhen Starcare Technology Co.,LTD.). Recoveries of the data obtained from the certified values for the purpose of quality control showed accuracies less than typical analytical errors (tolerances of 10%). The standard deviation of the analytical data from duplicate samples was less than 5%.

2.4. Statistical analysis and GIS

A multivariate statistical analysis was employed to identify the relationship between the variables and their potential sources using the PASW Statistic 18.0 software program. A correlation analysis of heavy metals usefully provided effective information to interpret heavy metal sources and pathways in the environment (Manta et al., 2002). Pearson's correlation matrix was applied to calculate correlation coefficients between the property variables (Rodríguez et al., 2009). Based on the results of the correlation analysis, a principal component analysis (PCA) was used to identify tracers of heavy metal natural enrichment and anthropogenic influence in the study area. In addition, Varimax rotation was used to reduce the dimensionality of the original data space to a few factors (Chen et al., 2008). To develop scatter diagrams, a curvilinear regression analysis was employed to determine the relationship between the heavy metal concentrations and distance to the Sb smelter. A Kolmogorov-Smirnov test was applied to assess the normality of the original data.

The Kriging interpolation method was applied to assess the degree of pollution (Kumar, 2015). The spatial interpolation and GIS mapping were employed to graphically and digitally present the

Table 1
Descriptive statistics for heavy metal concentrations and basic parameters in soils.

	Unit	Mean	Min	Max	CV (%)	S.D	K-S	Background value[a]
Cr	mg kg^{-1}	32.30	16.2	74.9	34.30	11.1	1.188*	54
Mn	mg kg^{-1}	399.98	59.4	1033.4	60.03	240.1	0.535*	601
Ni	mg kg^{-1}	18.77	7.0	37.4	38.75	7.3	0.925*	32
Cu	mg kg^{-1}	17.86	4.1	110.9	96.07	17.1	1.949	18
Zn	mg kg^{-1}	512.09	28.6	10,161.5	341.43	1748.4	3.173	101
As	mg kg^{-1}	40.46	3.3	426.1	171.31	69.3	2.172	14
Cd	mg kg^{-1}	7.56	0.1	154.2	327.36	24.7	3.162	0.11
Pb	mg kg^{-1}	45.43	9.5	405.4	135.09	61.3	2.397	38
Sb	mg kg^{-1}	273.67	1.5	3799.4	245.34	97.9	2.543	2.98
pH	–	5.50	2.85	7.46	27.73	1.5	1.125*	–
S	%	0.20	0.05	0.89	71.90	0.2	1.143	–

* Asymptotic significance >0.05 (2-tailed).
Min, minimum; Max, maximum; CV, coefficient of variation; S.D, standard deviation; K-S, Kolmogorov-Smirnov test.
[a] Background value of Hunan Province mountain soil (Li and Zheng, 1989).

spatial distribution maps of heavy metals in the study area. Spatial interpolation frequently uses the method of ordinary Kriging to estimate spatial data at unsampled locations (Altfelder et al., 2002). These analyses were performed using the AcrMap 9.3.

2.5. Geoaccumulation index (I_{geo})

Geoaccumulation indexes of single metals were calculated to determine the pollution degree using Muller's (1969) expression:

$$I_{geo} = \log_2\left(\frac{C_{Sample}}{1.5 \times C_{Background}}\right),$$

where C_{Sample} is the concentration of the metal examined in the samples, and $C_{Background}$ is the geochemical background concentration of that metal. A factor of 1.5 was introduced in this equation to correct the lithospheric effects in the background matrix. The geoaccumulation index consists of seven grades or classes. $I_{geo} \leq 0$ is class 0 (practically uncontaminated), $0 < I_{geo} \leq 1$ is class 1 (uncontaminated to moderately contaminated), $1 < I_{geo} \leq 2$ is class 2 (moderately contaminated), $2 < I_{geo} \leq 3$ is class 3 (moderately to heavily contaminated), $3 < I_{geo} \leq 4$ is class 4 (heavily contaminated), $4 < I_{geo} \leq 5$ is class 5 (heavily to extremely contaminated), and $5 < I_{geo}$ is class 6 (extremely contaminated).

3. Results and discussion

3.1. Physico-chemical characteristics

Descriptive statistics of the basic parameters and heavy metal concentrations in the soils are presented in Table 1 pH is related to the mobility and solubility of heavy metals in soils (Huang et al., 2012). Wide pH ranges (2.85–7.64) in soils may be associated with the influence of extrinsic factors at each sampling sites. Many factors (i.e., acidic mine drainage, tailings and acid rain) impact the pH of the soils surrounding the mining area. In general, the property parameters of the collected samples showed extensive variability in the study area. The coefficient of variation (CV) of S was 71.9%, which show moderate variability. However, the CV of Cu, Zn, As, Cd, Pb and Sb in the soils were 96.07%, 341.43%, 171.31%, 327.36%, 135.09% and 245.34%, respectively, which indicate high variability. Spatial variability is associated with natural or extrinsic factors (Zhao et al., 2010). The natural variability is mainly attributed to the weathering of parent materials, whereas the extrinsic variability is due to anthropogenic activities. The application of the K-S test confirmed that the distributions of Cu, Zn, As, Cd, Pb, Sb and S in the soils were not normally distributed, whereas Cr, Mn, Ni and pH were normally distributed.

The average concentrations of Zn, As, Cd, Pb and Sb in the soils were 512.09 mg kg^{-1}, 40.46 mg kg^{-1}, 7.56 mg kg^{-1}, 45.43 mg kg^{-1}, 273.67 mg kg^{-1}, respectively. These metal concentrations in the soils significantly exceeded their background values (101 mg kg^{-1} for Zn, 14 mg kg^{-1} for As, 0.11 for mg kg^{-1} Cd, 38 mg kg^{-1} for Pb and 2.98 mg kg^{-1} for Sb) on the Hunan Province scale (Li and Zheng, 1989). The higher concentrations and high variability of Zn, As, Cd, Pb and Sb indicate that they may be determined by extrinsic factors. The lower concentrations and moderate variability of Cr, Mn and Ni suggested that they may be controlled by natural factors. The average concentration of Cu in the soils was lower than the background values. Thus, the high variability of Cu could be influenced by natural and extrinsic factors.

Table 2
Pearson correlation coefficients for heavy metals and soil properties.

	Cr	Mn	Ni	Cu	Zn	As	Cd	Pb	Sb	pH	S
Cr	1										
Mn	0.461[b]	1									
Ni	0.684[b]	0.510[b]	1								
Cu	0.287[a]	0.466[b]	0.630[b]	1							
Zn	0.127	0.345[a]	0.493[b]	0.946[b]	1						
As	0.097	0.072	0.563[b]	0.604[b]	0.548[b]	1					
Cd	0.123	0.317[a]	0.527[b]	0.943[b]	0.984[b]	0.637[b]	1				
Pb	0.189	0.440[b]	0.436[b]	0.929[b]	0.925[b]	0.364[b]	0.897[b]	1			
Sb	−0.022	0.134	0.441[b]	0.664[b]	0.581[b]	0.801[b]	0.650[b]	0.535[b]	1		
pH	0.194	0.436[b]	0.405[b]	0.330[a]	0.273	0.236	0.294[a]	0.225	0.092	1	
S	0.250	0.017	0.484[b]	0.558[b]	0.540[b]	0.713[b]	0.613[b]	0.366[b]	0.444[b]	0.389[b]	1

[a] Correlation is significant at the 0.05 level.
[b] Correlation is significant at the 0.01 level.

Table 3
Total variance explained for heavy metal concentrations.

Component	Initial eigenvalues			Element	Rotated component		
	Total	% of variance	Cumulative %		PC1	PC2	PC3
1	5.371	59.676	59.676	Cr	−0.019	0.038	**0.924**
2	1.636	18.175	77.851	Mn	0.422	−0.176	**0.692**
3	1.051	11.677	89.528	Ni	0.250	0.490	**0.775**
4	0.502	5.582	95.110	Cu	**0.859**	0.391	0.292
5	0.229	2.542	97.653	Zn	**0.919**	0.320	0.114
6	0.139	1.547	99.200	As	0.255	**0.924**	0.098
7	0.041	0.457	99.657	Cd	**0.875**	0.426	0.109
8	0.022	0.248	99.904	Pb	**0.951**	0.143	0.173
9	0.009	0.096	100.000	Sb	0.421	**0.809**	−0.021

Extraction method: principal component analysis. The classification of heavy metals are clearly highlighted in bold.

3.2. *Inter-element relationships and possible sources*

To identify and characterize the inter-element relationships and their associations with soil properties (pH and S), a matrix of correlation coefficients was calculated by correlation analysis (Table 2). Zn exhibited positive and significant correlations with Ni, As, Sb, Cu, Pb and Cd ($r^2 = 0.493^{**}$-0.984^{**}) at a 0.01 significance level. The strong correlations among metals potentially indicate their common origins and similar pathways. Forghani et al. (2015) also reported similar results for potential toxic element mobilities around

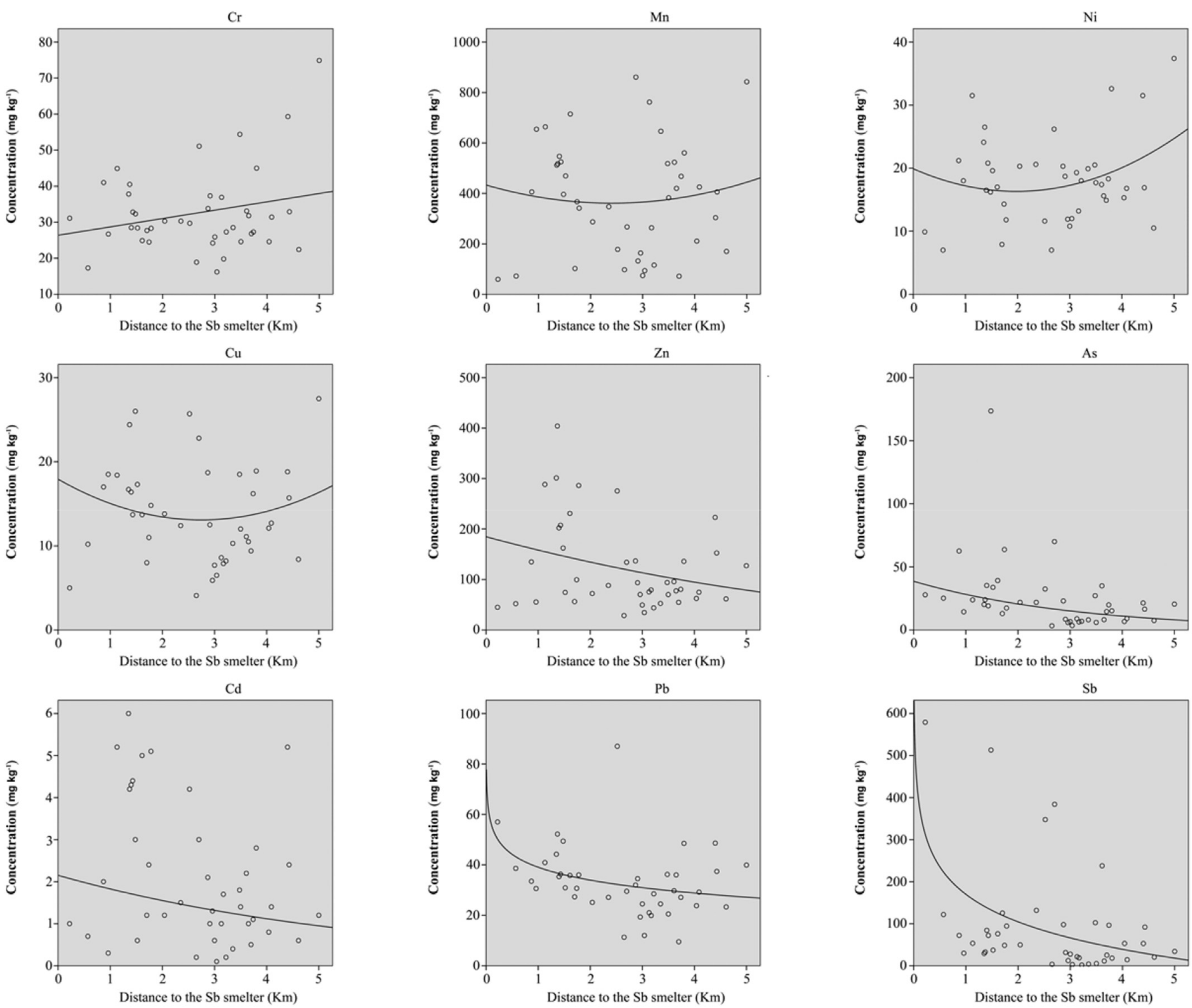

Fig. 2. Scatter diagrams of heavy metal concentrations and the increasing distance from Sb smelter.

a mining area. In addition, Sb also displayed a strong correlation with As ($r^2 = 0.801^{**}$), which could imply similar geochemical behaviors for the transport and deposition of Sb and As. The specific relationships could be associated with their similar chemical properties (Hong et al., 2012).

Usually, significant positive associations between heavy metals and soil properties can indicate similar origins. The significant correlation between the heavy metals and S ($r^2 = 0.366^{**}$-0.713^{**}), except for Cr and Mn, suggest that they originated from common minerals such as stibnite, sphalerite and galena. Mining operation emissions have been suggested to be a predominant factor that impacts the accumulation of heavy metal concentrations in soils (Csavina et al., 2012). As a result of smelting activities, heavy metals present in sulfide particles probably were transported over the entire area from their point of origin. No significant correlations were found between the majority of heavy metals (Cr, Zn, As, Pb and Sb) and pH. This may be due to the comprehensive influence of multiple factors around the mining area. Acidic mine drainage, tailings and acid rain may change the pH and distribution of heavy metals at different levels. Moreover, soil environment may also limit the correlation between pH and heavy metal concentration. A similar result was reported for mine-affected soils in Bangladesh (Bhuiyan et al., 2010).

The results of the principal component analysis showed three components with eigenvalues greater than 1.0 and that explained 89.5% of the data variation. According to the rotated component matrix (Table 3), the heavy metals were classified to identify the pollution sources.

More specifically, the first principal component (PC1) included Cu, Zn, Cd and Pb, and contributed 59.6% of the cumulative variance. The average concentrations of Zn, Cd and Pb in the soils were clearly higher than the background values. In addition, the significant correlations between S and these metals are indicative of an anthropogenic source for PC1. Cu, Zn, Cd and Pb may be released from sulfide minerals (sphalerite and galena) that were associated with the smelting processes. Sb and As were classified as the second principal component (PC2). In general, Sb is released to the atmosphere attached to fine particulates during high temperature processes of industrial production (Tian et al., 2014). The transport and deposition of fine particulates are controlled by the prevailing wind in smelting operation areas (Csavina et al., 2011). Therefore, Sb and As attached to fine particulates were spread over the study area. In addition, the high CV values of Sb and As confirmed the inhomogeneous distribution characteristic. The third principal component (PC3) contains Cr, Mn and Ni, which could be defined as a natural source. The relatively lower CV values showed the

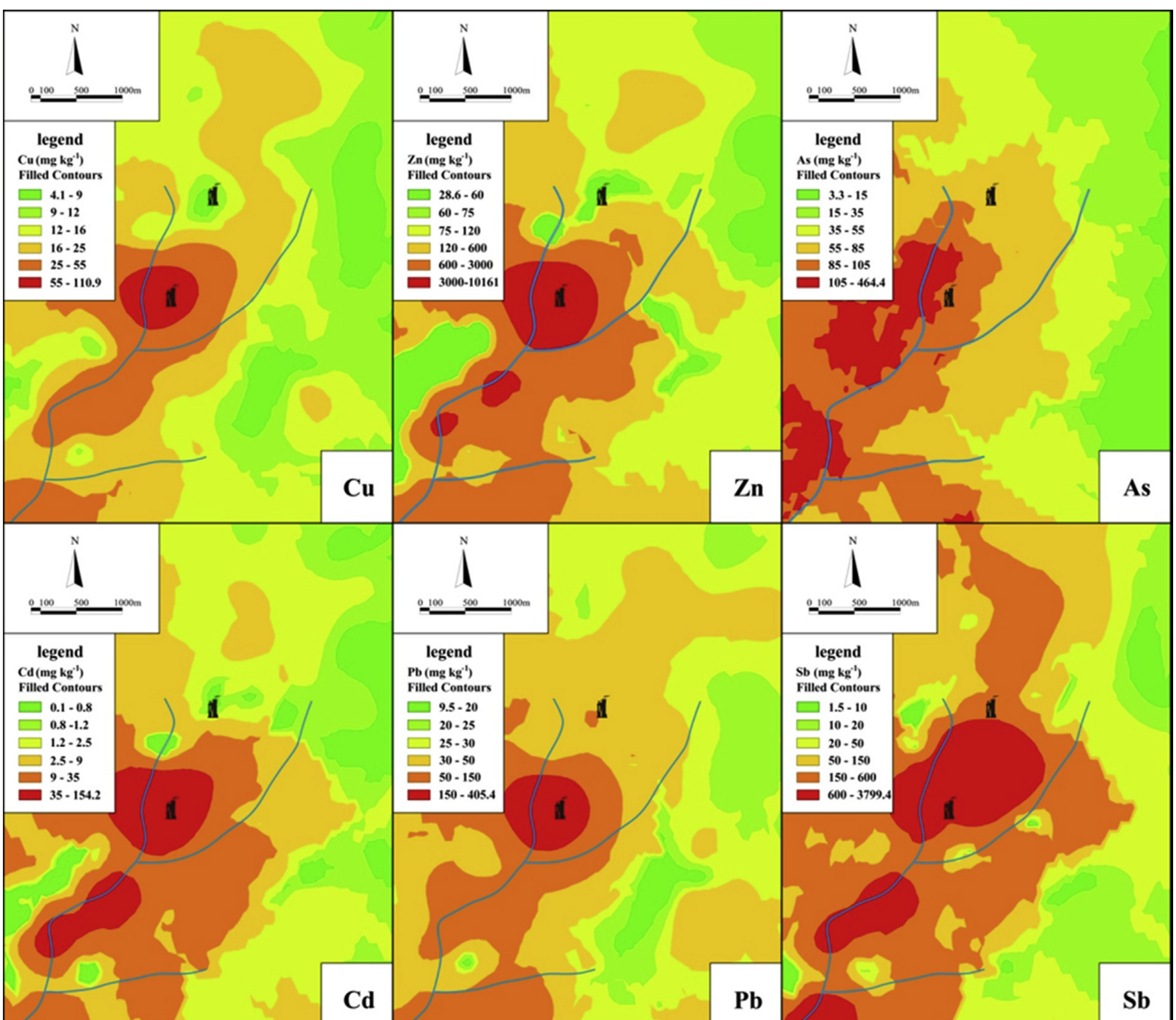

Fig. 3. Distribution characteristic maps of heavy metals (Cu, Zn, As, Cd, Pb and Sb) in soil over the study area.

uniform distributions of those metals in the study area. Moreover, the mean concentrations of Cr, Mn and Ni were below the background values, indicating PC3 was mainly influenced by natural factors.

To further reveal the influence of Sb smelting on the heavy metal sources, distance to the Sb smelter was used as an ancillary predictor. Scatter diagrams of heavy metals concentrations variation trends were constructed with increasing distance to the Sb smelter using a curvilinear regression analysis (Fig. 2). Gradually decreasing concentrations of Mn, Ni and Cu were found in the first 2 km from the smelter and increased slowly after that. The concentration of Cr increased slowly with increasing distance to the Sb smelter. The variation trends of the Cr, Mn, Ni and Cu concentrations may be caused by natural factors in the study area. As seen from Fig. 2, the variation trends showed a clear decline in heavy metal concentrations (Zn, As, Cd, Pb and Sb) with increasing distance from the Sb smelter. A similar result was observed in atmospheric metal depositions in a heavily polluted mining district (Castillo et al., 2013). The mobility of these metals may be the result of contaminant fume emissions and aeolian erosion.

3.3. Spatial distribution of heavy metals

Kriging interpolation was performed on all of the samples as a digital mapping method to obtain visual information on the spatial distributions of the heavy metals. According to the results, the impacted area and transport processes of the heavy metals were probably disclosed in the study area. Cr, Mn and Ni displayed smooth and regular distribution trends. The spatial distributions of Cr, Mn and Ni also showed an unclear relationship between their distribution trends and the Sb smelter. This may imply that their distributions were mainly attributed to natural factors such as the weathering and leaching of parent materials.

The gradually declining concentrations of heavy metals (Cu, Zn, As, Cd, Pb and Sb) showed similar distribution trends with increasing distance from the smelter (Fig. 3). This fact also indicates that contaminants were released from a common source. In the long term, the windborne transport and atmospheric deposition of dust may play a significant role in spreading contaminants (Zobeck and Van Pelt, 2006). These processes probably caused the differences in the metal spatial distribution patterns in the soils. It can be seen that the predominant wind directions are NW, WWN and NNE (Fig. S1, Electronic Supplementary Material), which coincided with the distribution trends of the heavy metal concentrations in the soils. The trends in the spatial distributions could be explained by the longer-term aeolian erosion of tailings and smelter fume emissions in the predominant wind directions.

The spatial maps of all the heavy metals showed common distribution trends, with relatively low concentrations in the eastern area. Vegetation coverage at the sampling sites (Fig. 1) could also influence the distribution of heavy metals in the soils. The average concentrations of the heavy metals showed significant differences in three vegetation coverage soils, with the exception of Cr, Mn and Ni (Table S1, Electronic Supplementary Material). Generally, heavy metal concentrations are easily affected by natural factors and human activities at the low vegetation coverage level in soils (Kabas et al., 2012). The lowest concentrations of heavy metals in the woodland soils reflected that their mobility and deposition could be blocked by trees.

In addition to the influence of heavy metal accumulations in soils, alluvial erosion and sediment transport processes are also important problems. Sediments are transported from the Lianxi River to the Zi River. In the Lianxi River, the concentrations of Sb were approximately 10 times higher than those upstream (Table S2, Electronic Supplementary Material). The significant increase in Sb concentrations may be derived from mine drainage. Ondrejková et al. (2013) also reported high concentrations of Sb in mine drainage adit outflows. Quantities of soluble and insoluble heavy metal contaminants are commonly derived from mine drainage, leaching and runoff erosion of tailings (Pandey et al., 2007). There was a sensitive area for migrants in a wetland ecosystem (Liu et al., 2015). Consequently, the ecological environment of the Lianxi River and Zi River could be unavoidably influenced by long-term heavy metal contaminants discharging into the river.

3.4. Environmental pollution degree assessment

To identify the degree of heavy metal environmental pollution and assess their potential risk, the single metal geography accumulation degree must be analyzed in detail. The geoaccumulation index (I_{geo}) evaluation values are summarized in Table S3 (Electronic Supplementary Material). The average values of I_{geo} increased in the following order: Mn (−1.51), Ni (−1.46), Cr (−1.40), Cu (−0.91), Pb (−0.75), Zn (−0.24), As (0), Cd (3.46) and Sb (3.76). Specifically, the average values of I_{geo} for Sb and Cd exceeded 3 and belong to the heavily contamination class. Therefore, the environment quality was obviously threatened by their accumulation in soils. However, some metals (Cr, Mn and Ni) in the soils exhibited a practically uncontaminated degree because of their low I_{geo} values in the study area. The wide range of I_{geo} values (Cu, Zn, As, Cd, Pb and Sb) indicate differences in their pollution degrees in the spatial region.

Additionally, the interpolated trend of the I_{geo} values for Sb is shown in Fig. 4. The map of the pollution degree evaluation results reveals a densely populated area along a stripe from the northwest towards the southwest (NNE - SW) through the study area. The pollution degree distribution was in accordance with the prevailing

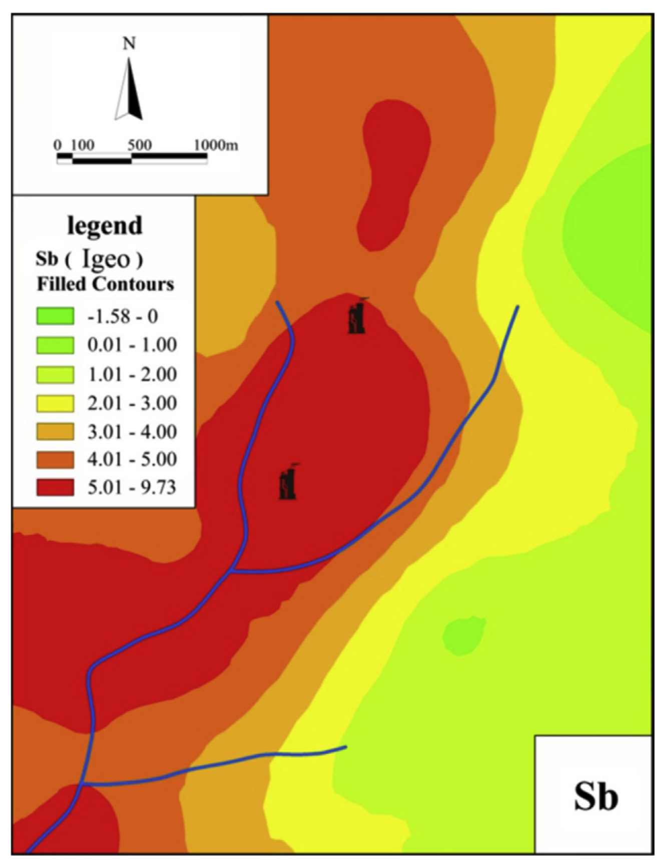

Fig. 4. Filled contours of geoaccumulation index value (I_{geo}) of Sb in soil over the study area.

wind direction, which can be attributed to the windborne transport and atmospheric deposition of contaminants. The environmental risk therefore could be seriously increased by heavy metal contaminants from the smelter and tailings.

4. Conclusion

The application of tools, methods and indices revealed the distribution characteristics of heavy metals in soils around an antimony mine area in central China. The results of the statistical analysis, correlation analysis and PCA allow two groups of heavy metals to be distinguished. The first group contains Cr, Mn and Ni, which are related to natural factors. The second group includes Cu, Zn, As, Cd, Pb and Sb, which are mainly derived from the smelter and tailings emissions. Spatial interpolation and the GIS mapping method were used to construct spatial distribution maps of heavy metals in the study area. The spatial distribution patterns of Cu, Zn, As, Cd, Pb and Sb illustrate the influences of wind, rivers, distance and vegetation coverage. The results also highlight that their spatial distribution trends coincide with the predominant wind direction. The environmental quality evaluation will serve as a basis for monitoring and protecting soils in the mine area.

Acknowledgments

This research was supported by the National Natural Science Foundation of China (51521006, 51579097).

Appendix A. Supplementary data

Supplementary data related to this article can be found at http://dx.doi.org/10.1016/j.chemosphere.2016.12.011.

References

Altfelder, Beyer, Duijnisveld, Schneider, Streck, 2002. Distribution of Cd in the vicinity of a metal smelter: interpolation of soil Cd concentrations with regard to regulative limits. J. Plant Nutr. Soil Sci. 165, 697–705.
Bhuiyan, M.A., Parvez, L., Islam, M.A., Dampare, S.B., Suzuki, S., 2010. Heavy metal pollution of coal mine-affected agricultural soils in the northern part of Bangladesh. J. Hazard. Mater. 173, 384–392.
Calace, N., Campisi, T., Iacondini, A., Leoni, M., Petronio, B.M., Pietroletti, M., 2005. Metal-contaminated soil remediation by means of paper mill sludges addition: chemical and ecotoxicological evaluation. Environ. Pollut. 136, 485–492.
Castillo, S., Rosa, J.D.d.l., Campa, A.M.S.d.l., González-Castanedo, Y., Fernández-Caliani, J.C., Gonzalez, I., Romero, A., 2013. Contribution ofmine wastes to atmospheric metal deposition in the surrounding area of an abandoned heavily polluted mining district (Rio Tinto mines, Spain). Sci. Total Envrion. 449, 363–372.
Chen, T., Liu, X., Zhu, M., Zhao, K., Wu, J., Xu, J., Huang, P., 2008. Identification of trace element sources and associated risk assessment in vegetable soils of the urban-rural transitional area of Hangzhou, China. Environ. Pollut. 151, 67–78.
Chopin, E.I.B., Alloway, B.J., 2007. Distribution and mobility of trace elements in soils and vegetation around the mining and smelting areas of Tharsis, Ríotinto and Huelva, Iberian pyrite belt, SW Spain. Water Air Soil Pollut. 182, 245–261.
Csavina, J., Field, J., Taylor, M.P., Gao, S., Landazuri, A., Betterton, E.A., Saez, A.E., 2012. A review on the importance of metals and metalloids in atmospheric dust and aerosol from mining operations. Sci. Total Envrion. 433, 58–73.
Csavina, J., Landazuri, A., Wonaschutz, A., Rine, K., Rheinheimer, P., Barbaris, B., Conant, W., Saez, A.E., Betterton, E.A., 2011. Metal and metalloid contaminants in atmospheric aerosols from mining operations. Water Air Soil Pollut. 221, 145–157.
de Souza, J.J., Abrahao, W.A., de Mello, J.W., da Silva, J., da Costa, L.M., de Oliveira, T.S., 2015. Geochemistry and spatial variability of metal(loid) concentrations in soils of the state of Minas Gerais, Brazil. Sci. Total Envrion. 505, 338–349.
Dragović, S., Mihailović, N., Gajić, B., 2008. Heavy metals in soils: distribution, relationship with soil characteristics and radionuclides and multivariate assessment of contamination sources. Chemosphere 72, 491–495.
Forghani, G., Mokhtari, A.R., Kazemi, G.A., Fard, M.D., 2015. Total concentration, speciation and mobility of potentially toxicelements in soils around a mining area in central Iran. Chem. Erde Geochem 75, 323–334.
Fu, Z., Wu, F., Mo, C., Deng, Q., Meng, W., Giesy, J.P., 2016. Comparison of arsenic and antimony biogeochemical behavior in water, soil and tailings from Xikuangshan, China. Sci. Total Envrion. 539, 97–104.
Hong, S., Soyol-Erdene, T.O., Hwang, H.J., Hong, S.B., Hur, S.D., Motoyama, H., 2012. Evidence of global-scale As, Mo, Sb, and Tl atmospheric pollution in the antarctic snow. Environ. Sci. Technol. 46, 11550–11557.
Huang, L.M., Deng, C.B., Huang, N., Huang, X.J., 2012. Multivariate statistical approach to identify heavy metal sources in agricultural soil around an abandoned Pb–Zn mine in Guangxi Zhuang Autonomous Region, China. Environ. Earth Sci. 68, 1331–1348.
ISO11047, 1998. Soil Quality - Determination of Cadmium, Chromium, Cobalt, Copper, Lead, Manganese, Nickel and Zinc - Flame and Electrothermal Atomic Absorption Spectrometric Methods. International Standard Organization, Geneva, Switzerland.
Kabas, S., Faz, A., Acosta, J.A., Zornoza, R., Martínez-Martínez, S., Carmona, D.M., Bech, J., 2012. Effect of marble waste and pig slurry on the growth of native vegetation and heavy metal mobility in a mine tailing pond. J. Geochem. Explor. 123, 69–76.
Kim, C.S., Anthony, T.L., Goldstein, D., Rytuba, J.J., 2014. Windborne transport and surface enrichment of arsenic in semi-arid mining regions: examples from the Mojave Desert, California. Aeolian Res. 14, 85–96.
Křibek, B., Majer, V., Pašava, J., Kamona, F., Mapani, B., Keder, J., Ettler, V., 2014. Contamination of soils with dust fallout from the tailings dam at the Rosh Pinah area, Namibia: regional assessment, dust dispersion modeling and environmental consequences. J. Geochem. Explor. 144, 391–408.
Kumar, S., 2015. Estimating spatial distribution of soil organic carbon for the Midwestern United States using historical database. Chemosphere 127, 49–57.
Li, J., Zheng, C., 1989. Manual Data for Environmental Background Value. China Environmental Science Press, Beijing.
Li, Z., Feng, X., Li, G., Bi, X., Zhu, J., Qin, H., Dai, Z., Liu, J., Li, Q., Sun, G., 2013. Distributions, sources and pollution status of 17 trace metal/metalloids in the street dust of a heavily industrialized city of central China. Environ. Pollut. 182, 408–416.
Liu, F., Le, X.C., McKnight-Whitford, A., Xia, Y., Wu, F., Elswick, E., Johnson, C.C., Zhu, C., 2010. Antimony speciation and contamination of waters in the Xikuangshan antimony mining and smelting area, China. Environ. Geochem Health 32, 401–413.
Liu, J., Liang, J., Yuan, X., Zeng, G., Yuan, Y., Wu, H., Huang, X., Liu, J., Hua, S., Li, F., Li, X., 2015. An integrated model for assessing heavy metal exposure risk to migratory birds in wetland ecosystem: a case study in Dongting Lake Wetland, China. Chemosphere 135, 14–19.
Müller, G., 1969. Index of geoaccumulation in sediments of the rhine river. Geojournal 2, 108–118.
Manta, D.S., Angelone, M., Bellanca, A., Neri, R., Sprovieri, M., 2002. Heavy metals in urban soils: a case study from the city of Palermo (Sicily), Italy. Sci. Total Envrion. 300, 229–243.
Okkenhaug, G., Zhu, Y.G., Luo, L., Lei, M., Li, X., Mulder, J., 2011. Distribution, speciation and availability of antimony (Sb) in soils and terrestrial plants from an active Sb mining area. Environ. Pollut. 159, 2427–2434.
Ondrejková, I., Ženišová, Z., Fľaková, R., Krčmář, D., Sracek, O., 2013. The distribution of antimony and arsenic in waters of the Dúbrava abandoned mine site, Slovak Republic. Mine Water Environ. 32, 207–221.
Pandey, P.K., Sharma, R., Roy, M., Pandey, M., 2007. Toxic mine drainage from Asia's biggest copper mine at Malanjkhand, India. Environ. Geochem Health 29, 237–248.
Qi, C., Wu, F., Deng, Q., Liu, G., Mo, C., Liu, B., Zhu, J., 2011. Distribution and accumulation of antimony in plants in the super-large Sb deposit areas, China. Microchem J. 97, 44–51.
Rodríguez, L., Ruiz, E., Alonso-Azcárate, J., Rincón, J., 2009. Heavy metal distribution and chemical speciation in tailings and soils around a Pb–Zn mine in Spain. J. Environ. Manage 90, 1106–1116.
Sajn, R., 2006. Factor analysis of soil and attic-dust to separate mining and metallurgy influence, Meza valley, Slovenia. Math. Geol. 38, 735–747.
Sun, C., Liu, J., Wang, Y., Sun, L., Yu, H., 2013. Multivariate and geostatistical analyses of the spatial distribution and sources of heavy metals in agricultural soil in Dehui, Northeast China. Chemosphere 92, 517–523.
Szolnoki, Z., Farsang, A., Puskas, I., 2013. Cumulative impacts of human activities on urban garden soils: origin and accumulation of metals. Environ. Pollut. 177, 106–115.
Tian, H., Zhou, J., Zhu, C., Zhao, D., Gao, J., Hao, J., He, M., Liu, K., Wang, K., Hua, S., 2014. A comprehensive global inventory of atmospheric Antimony emissions from anthropogenic activities, 1995-2010. Environ. Sci. Technol. 48, 10235–10241.
Wang, X., He, M., Xi, J., Lu, X., 2011. Antimony distribution and mobility in rivers around the world's largest antimony mine of Xikuangshan, Hunan Province, China. Microchem J. 97, 4–11.
Yang, D., Shimizu, M., Shimazaki, H., Li, X., Xie, Q., 2006. Sulfur isotope geochemistry of the supergiant Xikuangshan Sb deposit, central Hunan, China: constraints on sources of ore constituents. Resour. Geol. 56, 385–396.
Yang, H., He, M., Wang, X., 2015. Concentration and speciation of antimony and arsenic in soil profiles around the world's largest antimony metallurgical area in China. Environ. Geochem Health 37, 21–33.
Zhao, K., Liu, X., Xu, J., Selim, H.M., 2010. Heavy metal contaminations in a soil-rice system: identification of spatial dependence in relation to soil properties of paddy fields. J. Hazard. Mater. 181, 778–787.
Zobeck, T.M., Van Pelt, R.S., 2006. Wind-induced dust generation and transport mechanics on a bare agricultural field. J. Hazard. Mater. 132, 26–38.